J. Fluid Mech. (1979), *vol.* 95, *part* 4, *pp.* 761–777
Printed in Great Britain

Heat transfer in transient and unsteady flows past a heated circular cylinder in the range $1 \leqslant R \leqslant 40$

By C. J. APELT AND M. A. LEDWICH
Department of Civil Engineering, University of Queensland, Australia

(Received 6 December 1977 and in revised form 29 January 1979)

The response of a heated circular cylinder to impulsive and sinusoidal variations in the velocity of flow past it has been simulated by numerical integration of the governing equations. The fluid has been treated as viscous and incompressible and as having constant properties. The range of Reynolds number investigated was $1 \leqslant R \leqslant 40$. Since vortex shedding normally does not occur in this range, the flows were treated as symmetrical. The thermal and flow transients are presented for the following cases.:

(i) impulsive starts from rest to final steady state Reynolds numbers 1, 5, 10, 26·67;

(ii) impulsive increases in velocities of 50 % magnitude from steady state Reynolds numbers 1, 10 and 26·67;

(iii) sinusoidal variation in velocity with amplitude of 10 % impressed on a mean flow at Reynolds number 10.

Results are also given for the thermal transients associated with instantaneous changes in cylinder temperature at Reynolds numbers 1, 5 and 40. The results obtained for transient and steady state flow parameters are in agreement with those obtained numerically and experimentally by other workers and the results for steady state heat flux from the cylinder are in agreement with experimental values. The new results obtained for heat transfer in unsteady flows provides information which is relevant to the operation of hot-wire anemometers.

1. Introduction

Theoretical studies of the heat transfer from a heated circular cylinder in a flowing fluid have been carried out by a number of authors. Cole & Roshko (1954), Levey (1959), Illingworth (1963), Kassoy (1967) and Wood (1968) used the Oseen approximation while Hieber & Gebhart (1968) and Hodnett (1969) used the method of matched asymptotic expansions. In all of these studies, it is required that the Reynolds number R tend to zero; the highest order results, those of Wood and of Hieber & Gebhart, give values for the Nusselt number which correlate with the experimental data of Collis & Williams (1959) within 3 % for $R < 0{\cdot}4$. The only theoretical study we know which deals with unsteady heat transfer at low Reynolds numbers is that of Davies (1976) who used an Oseen approximation of the energy equation to estimate the fluctuating heat transfer from a heated cylinder at $R \ll 1$.

Many numerical solutions of impulsively started flow past a circular cylinder have been reported since the first was completed by Payne (1958). Most of these were carried out for small values ($\leqslant 100$) of the final steady state Reynolds number and it is

0022-1120/79/4352-7950 $02.00

surprising that none included any computation of heat transfer from the cylinder. The only work published on numerical calculation of heat transfer from a cylinder in flows at low Reynolds numbers prior to that reported in this paper is that of Dennis, Hudson & Smith (1968) and this was restricted to steady flows.

The numerical solutions reported below were computed in order to provide a reasonably detailed description of the heat transfer characteristics of a heated circular cylinder in unsteady flows at Reynolds numbers in the range in which vortex shedding does not normally occur, i.e. $R \leqslant 40$. The details of heat transfer and of fluid dynamic functions have been obtained for the following cases:

(i) impulsive start from rest to final steady state Reynolds numbers of 1, 5, 10 and 26·67, with the cylinder temperature held constant;

(ii) impulsive increases in velocity of 50 % magnitude from steady state Reynolds numbers 1, 10 and 26·67, with the cylinder temperature held constant;

(iii) sinusoidal variation in velocity impressed on a mean flow at a Reynolds number of 10, with the cylinder temperature held constant.

In addition the response of heat transfer to changes in cylinder temperature while the flow is steady was computed for instantaneous increases in cylinder temperature in flows at Reynolds numbers of 1, 5 and 40.

The results of the numerical solutions provide new data concerning the heat transfer from a heated cylinder in impulsively started flow, the response of heat transfer and of fluid dynamic functions for a heated cylinder in unsteady flow and the heat transfer transients when the temperature of a cylinder in steady flow is changed suddenly. In addition to the fundamental value this information possesses in itself, it provides data which can be used for the development of a mathematical model of a complete hot-wire anemometer system. The construction of such a model has been described by Bullock & Ledwich (1973).

2. Mathematical model

In the numerical solutions we consider two-dimensional flow of an incompressible fluid with constant viscosity and thermal conductivity past a circular cylinder of negligible thermal inertia. The effects of heating of the fluid by viscous dissipation and of radiation from the cylinder are neglected.

With the foregoing assumptions, the Navier–Stokes equation for the fluid motion can be expressed in the form of the vorticity-transport equation

$$\frac{\partial \zeta}{\partial t}+\frac{\partial (u\zeta)}{\partial x}+\frac{\partial (v\zeta)}{\partial y}=\frac{2}{R}\nabla^2\zeta \tag{1}$$

in which all quantities have been made dimensionless by scaling with respect to the radius of the cylinder a, and the velocity of the approach stream U. In the equation (1), u and v are the Cartesian components of the velocity vector in the x and y directions, respectively, ζ is the vorticity and the Reynolds number, R, is $2Ua/\nu$, where ν is the kinematic viscosity. The dimensionless quantities in equation (1) are related to dimensional quantities, indicated with a prime, as follows:

$$x = x'/a; \quad u = u'/U; \quad t = t'U/a; \quad \zeta = \zeta' a/U.$$

Introduction of the stream function, ψ, such that $u = \partial\psi/\partial y$, $v = -\partial\psi/\partial x$, leads to the relation

$$\nabla^2\psi = -\zeta. \tag{2}$$

The energy equation can be expressed as

$$\frac{\partial T}{\partial t} + \frac{\partial(uT)}{\partial x} + \frac{\partial(vT)}{\partial y} = \frac{2}{RPr}\nabla^2 T \tag{3}$$

which is of the same form as the vorticity transport equation. The dimensionless temperature, T, is defined as $(T' - T'_\infty)/(T'_w - T'_\infty)$, where T'_∞ is the temperature of the approach stream, T'_w is the temperature of the cylinder, Pr, the Prandtl number, is ν/κ, and κ is the thermal diffusivity of the fluid. The value assigned to Pr is that conventionally used for air, 0·7. The boundary conditions which solutions of the governing equations (1), (2) and (3) must satisfy are

$$u = 0, \quad v = 0, \quad T = 1 \quad \text{at} \quad r = 1; \tag{4a}$$

$$u = 1, \quad v = 0, \quad T = 0 \quad \text{at} \quad r \to \infty. \tag{4b}$$

The effects of buoyancy are neglected in equation (1); the experimental studies of Collis & Williams (1959) showed that this is a valid approximation if $R > G^{\frac{1}{2}}$, where G is the Grashof number, $\beta\Delta T' g d^3/\nu^2$, in which β is the coefficient of thermal expansion of the fluid, $\Delta T'$ is a measure of the magnitude of temperature differences in the fluid, g is the acceleration due to gravity and d is the diameter of the cylinder. The use of the stream function implies that rates of change of density of the fluid due to changes in temperature are negligibly small so that the mass-conservation equation reduces to the statement that the velocity field is solenoidal. In the present context this approximation is valid if $(\beta\Delta T'\kappa)/(UL) \ll 1$ (Batchelor 1967). For air over a wide range of temperatures the inequality can be expressed approximately in the S.I. unit system, as $\Delta T'/R \ll 200$, provided that the length scales for velocity gradients and for temperature gradients are of the same order; this was found to be the case for the range of R considered in this paper. Use of no-slip boundary conditions at the surface of the cylinder implies that d is large compared to the mean free path in the fluid.

3. Numerical solution

3.1. *Co-ordinate transformation*

In order to simplify treatment of the normal gradient conditions at the surface of the cylinder the numerical solutions were computed in a transformed co-ordinate system defined by

$$\xi = -k\theta, \quad \eta = k\ln r,$$

where θ and r are polar co-ordinates and k, a scale factor, is related to the number of integral subdivisions of the complete circumference of the cylinder ($2n$) by $k = n/\pi$. In the transformed co-ordinate system the governing equations take the form,

$$\frac{\partial\zeta}{\partial t} + \left(\frac{k}{r}\right)^2 \frac{\partial(\zeta,\psi)}{\partial(\xi,\eta)} = \frac{2}{R}\left(\frac{k}{r}\right)^2 \nabla_{\xi\eta}\zeta, \tag{1a}$$

$$\nabla^2_{\xi\eta}\psi = -\zeta \Big/ \left(\frac{k}{r}\right)^2, \tag{2a}$$

$$\frac{\partial T}{\partial t} + \left(\frac{k}{r}\right)^2 \frac{\partial(T,\psi)}{\partial(\xi,\eta)} = \frac{2}{RPr}\left(\frac{k}{r}\right)^2 \nabla^2_{\xi\eta} T. \tag{3a}$$

3.2. *Finite difference approximations*

The equations (1a) and (3a) were integrated by the Alternating Direction Implicit (A.D.I.) method, with the convective terms discretized in a manner that, in itself, conserves kinetic energy so that there is no false dissipation introduced as a result of the discretization of these terms. As pointed out by Arakawa (1966), such discretization also avoids nonlinear instability which has its origin in space-truncation errors, a necessary requirement for successful numerical integration over long times. This choice of method was based on previous extensive comparative studies which showed that it possesses good accuracy and satisfactory economy in the context of the present application.

Each complete step of integration in time of the equations (1a) and (3a) consisted of two half steps, each of length δt, and the finite difference approximations to the equation (1a) for the pair of half steps are

$$\frac{1}{\delta t}(\zeta_{i,j}^{m+1}-\zeta_{i,j}^{m})+\frac{A_{ij}}{4}[(\psi_{i+1,j+1}^{m}-\psi_{i+1,j-1}^{m})\,\zeta_{i+1,j}^{m+1}$$
$$-(\psi_{i-1,j+1}^{m}-\psi_{i-1,j-1}^{m})\,\zeta_{i-1,j}^{m+1}-(\psi_{i+1,j+1}^{m}-\psi_{i-1,j+1}^{m})\,\zeta_{i,j+1}^{m}+(\psi_{i+1,j-1}^{m}-\psi_{i-1,j-1}^{m})\,\zeta_{i,j-1}^{m}]$$
$$=\frac{2A_{i,j}}{R}[(\zeta_{i+1,j}^{m+1}-2\zeta_{i,j}^{m+1}+\zeta_{i-1,j}^{m+1})+(\zeta_{i,j+1}^{m}-2\zeta_{i,j}^{m}+\zeta_{i,j-1}^{m})], \tag{5a}$$

$$\frac{1}{\delta t}(\zeta_{i,j}^{m+2}-\zeta_{i,j}^{m+1})+\frac{A_{ij}}{4}[(\psi_{i+1,j+1}^{m}-\psi_{i+1,j-1}^{m})\,\zeta_{i+1,j}^{m+1}$$
$$-(\psi_{i-1,j+1}^{m}-\psi_{i-1,j-1}^{m})\,\zeta_{i-1,j}^{m+1}-(\psi_{i+1,j+1}^{m}-\psi_{i-1,j+1}^{m})\,\zeta_{i,j+1}^{m+2}+(\psi_{i+1,j-1}^{m}-\psi_{i-1,j-1}^{m})\,\zeta_{i,j-1}^{m+2}]$$
$$=\frac{2A_{i,j}}{R}[(\zeta_{i+1,j}^{m+1}-2\zeta_{i,j}^{m+1}+\zeta_{i-1,j}^{m+1})+(\zeta_{i,j+1}^{m+2}-2\zeta_{i,j}^{m+2}+\zeta_{i,j-1}^{m+2})], \tag{5b}$$

in which $\zeta_{i,j}^{m}$ denotes $\zeta(i\delta\xi, j\delta\eta, m\delta t)$ and $A_{i,j}$ denotes $(k/hr_{i,j})^2$ where $h=\delta\xi=\delta\eta$, is the interval of spatial resolution in the transformed co-ordinates. The truncation error for the system of equations (5a) and (5b) is $O(\delta t^2)+O(h^2)$ for $R\geqslant 1$. The finite difference approximations for the numerical integration of (3a) are similar to those given above for the integration of (1a).

The equation (2a) was approximated by central differences, with truncation error $O(h^2)$, and the solution of the resulting set of simultaneous difference equations was computed with the Successive Over Relaxation (S.O.R.) process, using the optimum accelerator.

3.3. *Boundary conditions*

All of the numerical solutions were computed in the range of R for which vortex shedding does not normally occur and the flow is symmetric. This fact was used to limit the computations to one half of the flow field by the application of symmetry conditions along the radii corresponding to $\theta=0$ and π.

At the surface of the cylinder ($r=1$, $\eta=0$) the conditions applied were $\psi=0$, $T=1$ or as specified, for cases in which the temperature of the cylinder itself was varied. The values of ζ on the surface of the cylinder were calculated from the expression

$$\zeta_{i,0}=-3A_{i,0}\psi_{i,1}-\tfrac{1}{2}\zeta_{i,1}A_{i,0}/A_{i,1} \tag{6}$$

which incorporates the no-slip condition with truncation error $O(h^2)$.

In a numerical solution it is not possible to satisfy exactly the boundary conditions for $r \to \infty$ and some approximation to them must be imposed at a large but finite radius. Some authors have simply imposed the uniform flow conditions, (4*b*), at finite distance from the cylinder. However, Apelt (1958) and Takaisi (1969) have demonstrated that this simple procedure is unsatisfactory and leads to substantial inaccuracies unless the radial distance at which the conditions (4*b*) are imposed is very large, of order 100 times the radius of the cylinder. The numerical solutions described here had to be completed within a modest amount of computer time and it was necessary, for this reason, to limit the computational domain to one considerably smaller than that for which the conditions (4*b*) could be used. Some authors, e.g. Kawaguti (1953), Keller & Takami (1966) and Takami & Keller (1969), have dealt with this problem, for the case of steady flows, by using the asymptotic expressions for ψ and ζ obtained by Imai (1951) from the Oseen approximation to the Navier–Stokes equation. This procedure was not used here because our interest was essentially in calculation of unsteady flows and Imai's result is valid only for steady flow and, further, his result is strictly valid only for small values of R at the distances from the cylinder where the boundary conditions have to be applied in the numerical solutions. The approach adopted was to specify, at the outer limits of the numerical solution domain, values of the gradients in the radial direction of ζ and T which are consistent with Imai's asymptotic result. This procedure is similar to that used for steady flows by Apelt (1958) in solving the Navier–Stokes equation and by Dennis, Hudson & Smith (1968) in solving the energy equation. Use of the first term of Imai's asymptotic expression for ζ at large r leads to the relationship, for flow in the positive x direction,

$$\zeta(r_2, \theta)/\zeta(r_1, \theta) = (r_1/r_2)^{\frac{1}{2}} \exp\left[\tfrac{1}{2}R(r_1 - r_2)\sin^2\tfrac{1}{2}\theta\right]. \tag{7}$$

To the same order of approximation, the Oseen solution of the energy equation leads to the relationship,

$$T(r_2, \theta)/T(r_1, \theta) = (r_1/r_2)^{\frac{1}{2}} \exp\left[\tfrac{1}{2}RPr(r_1 - r_2)\sin^2\tfrac{1}{2}\theta\right]. \tag{8}$$

The expression (8) is equivalent to that used by Dennis, Hudson & Smith (1968). Use of the gradient conditions for ζ and T at large r given in (7) and (8) avoids constraining these quantities to incorrect values while ensuring that their spatial distribution will be generally in conformity with that given by the Oseen approximation. The values assigned to ψ at large r were those for the uniform stream. This is not consistent with equation (7) but computational tests indicated that the accuracy of the numerical solutions so obtained were satisfactory nevertheless, despite the acknowledged lack of elegance in the treatment of the boundary conditions for ψ.

3.4. *Some numerical details*

Previous numerical experiments had shown that the maximum value which can be used for the half time step, δt, in the integration of the equations (5) without encountering instability is approximately the same as that which would apply to the complete time step in the explicit method for integrating the same equations. If the spatial resolution is such that there are $2n$ intervals of subdivision of the complete circumference of the cylinder, the stability condition can be expressed as $\delta t < 0{\cdot}125R(\pi/n)^2$. The numerical experiments also had confirmed that good accuracy is achieved if the time step used is close to the limit for stability. Consequently, in all cases except where

otherwise noted, δt was set at a value which was 10 to 20 % smaller than the stability limit. Numerical tests confirmed that the results obtained for unsteady flow calculations with this value of δt were virtually identical at the same times as those computed with δt set at the stability limit.

In the cases of impulsive starts from rest, our chief interest was in the final steady state values, both in themselves and also as providing the initial conditions from which various transients were to begin. The computing budget available provided for a total of only $6\frac{1}{2}$ h on an IBM 360/50H computer (cycle time 2 μs) and, in order to reduce the amount of computing required to produce steady state values from impulsive starts, a simple stratagem was used with very satisfactory results. This involved computing an impulsive start through to steady state values at a coarser spatial discretization than that required for fine accuracy; interpolation was then applied to produce an approximate steady state solution at the finer discretization and this was used as the starting point for the final computation of the accurate steady state values. In most cases, the coarser discretization used was only twice as coarse as the final one but, even so, the computational effort required to produce the final steady state values was reduced to approximately one-tenth that which would have been required if the impulsive start had been computed from the beginning at the finer resolution. The results presented here have been obtained at a final spatial resolution such that $n = 20$, i.e. there were 40 intervals in the complete circumference of the cylinder, unless otherwise stated. The boundary conditions (7) and (8) were applied at $r = 23{\cdot}14$.

The solution of the finite difference equations derived from equation ($2a$) was computed to an absolute precision better than 10^{-4} at each time step.

4. Numerical results

4.1. *Steady state flow quantities*

A selection of the results obtained at steady states is presented in figures 1 to 3 to provide an indication of the accuracy achieved with the numerical solutions. In assessing the accuracy of our solutions we are now able to make use, in retrospect, of material published after our work was completed. The most significant of this is contained in the careful numerical solutions by Nieuwstadt & Keller (1973) of the steady state form of equations (1) and (2) and in the meticulously obtained experimental data of Coutanceau & Bouard (1977).

In figure 1 the values we calculated for the total drag coefficient, C_{Dt}, are shown to be in close agreement with those obtained by Nieuwstadt & Keller and also with those of Collins & Dennis (1973) and of Dennis & Chang (1970) for values of R from 5 to 40. Over this range all of the numerical results fall close to the mean line of the experimental results of Tritton (1959). At $R = 1$ our value of C_{Dt} lies at the upper range of Tritton's data while the result of Nieuwstadt & Keller lies at the lower range of the experimental data. Our results for the separate contributions from pressure drag and friction drag expressed as the coefficients C_{Dp} and C_{Df} are in close agreement with those of Collins & Dennis and of Dennis & Chang.

The length of the wake bubble, L, in our calculations is compared in figure 2 with the results for zero blockage which Coutanceau & Bouard inferred from their experimental data. The agreement between the two sets of results is very close at all values

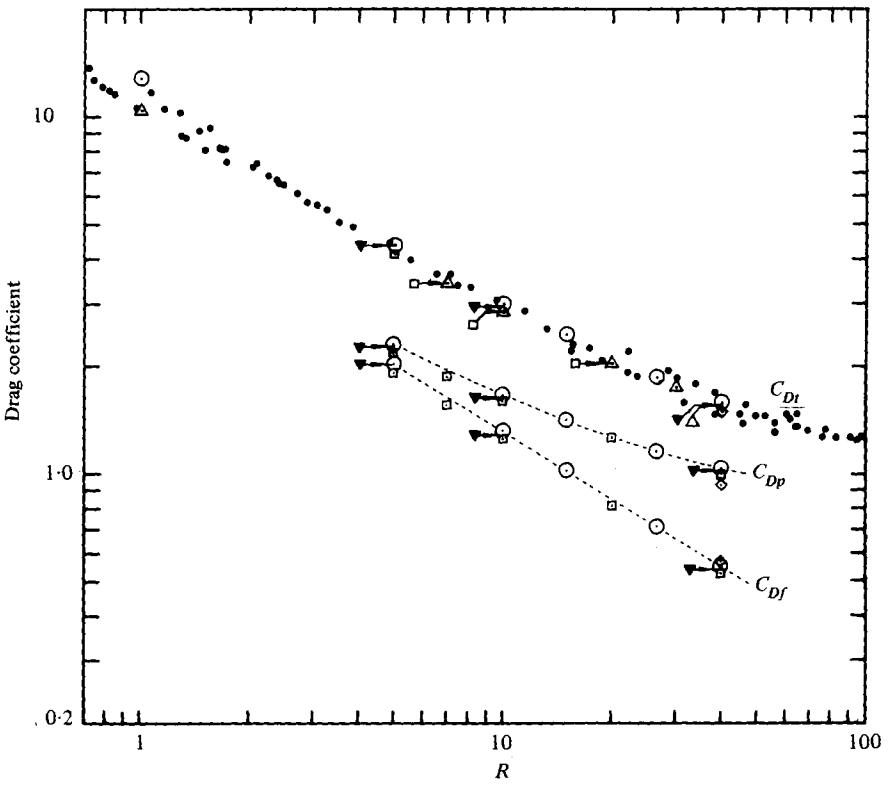

FIGURE 1. Variation of drag coefficient with Reynolds number. Experimental data: ●, Tritton (1959). Numerical solutions: ○, this study; △, Nieuwstadt & Keller (1973); ⊡, Dennis & Chang (1970); ▼, Collins & Dennis (1973); ◇, Apelt (1958).

of R. The independent numerical results of Nieuwstadt & Keller, of Collins & Dennis and of Dennis & Chang are also in close agreement with ours except for the rather large value of L obtained by the latter authors at $R = 40$. The results obtained for separation angle, θ_s, are also shown in figure 2. Our results are closer to those of Coutanceau & Bouard for zero blockage than are those of the other numerical studies for values of R less than 30. At $R = 40$ our result is somewhat larger than that of Coutanceau & Bouard which is in closer agreement with the results from the other numerical solutions. The magnitude and location of the maximum reverse velocity in the wake bubble are shown in figure 3. Our results for the magnitude of the maximum reverse velocity are in excellent agreement with those of Coutanceau & Bouard at all values of R, and our locations of the maxima are in close agreement with those of the same authors for all values of R less than 30. There is insufficient experimental data to provide confident determination of an experimental value for this location at $R = 40$ but it would appear that our result for this case is a little low and that that of Nieuwstadt & Keller may be the more accurate.

The comparisons in figures 1 to 3 show that our results for steady state quantities are in excellent agreement with the experimental data for the range $5 \leqslant R \leqslant 26{\cdot}67$ and, in this range, they appear to be at least as accurate as the best of the other numerical results. Beyond this range, i.e. at values of R of 1 and 40 the accuracy of

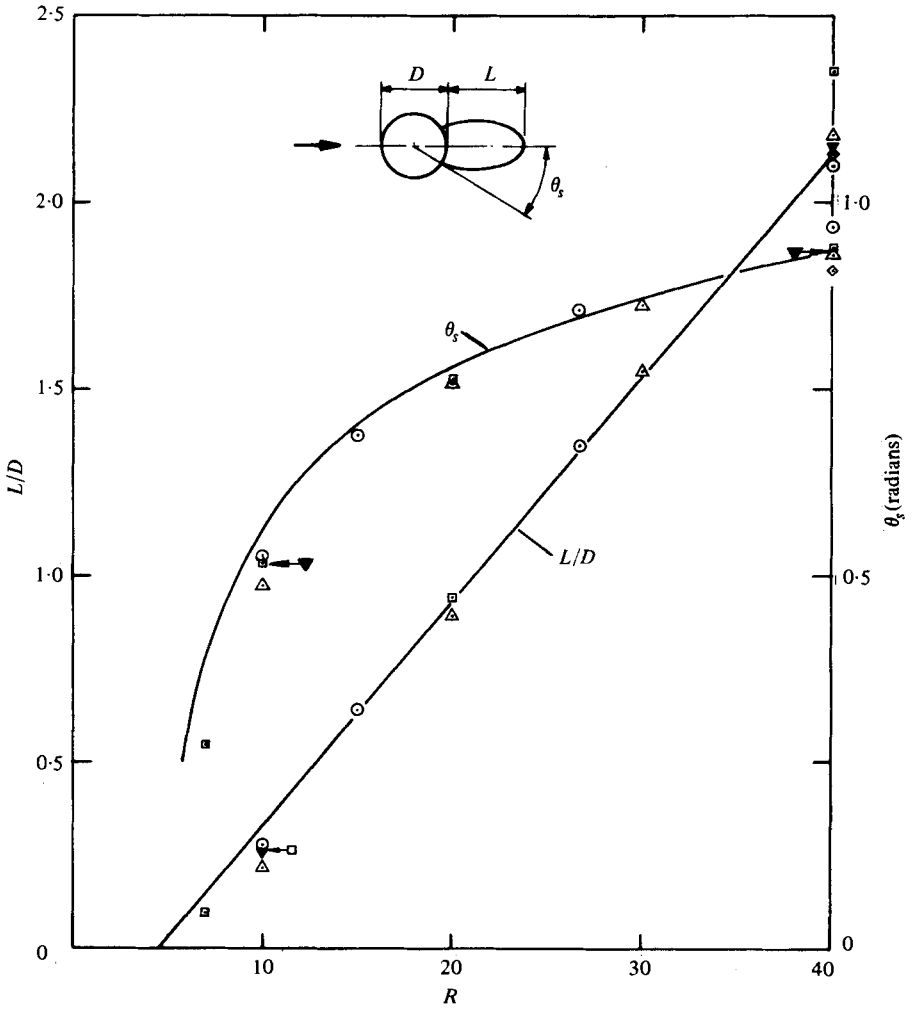

FIGURE 2. Length of closed wake bubble and separation angle. Experimental results: ——, Coutanceau & Bouard (1977). Numerical solutions: ⊙, this study; △, Nieuwstadt & Keller (1973); □, Dennis & Chang (1970); ▼, Collins & Dennis (1973); ◇, Apelt (1958).

our results is not quite so good but it is still quite sufficient for the purposes of the study, taking into account the limitations of the mathematical model discussed in § 2.

4.2. *Steady state heat transfer*

The variation with R of the heat transfer from the cylinder at steady state conditions is shown in figure 4. The heat transfer is expressed in non-dimensional terms as the Nusselt number Nu, defined as

$$Nu = \frac{1}{2\pi}\int_0^{2\pi} -2(\partial T/\partial r)_{r=1}\, d\theta. \tag{9}$$

Our results for Nu are compared with the experimental data of Collis & Williams (1959) and the results of the numerical solutions of Dennis *et al.* (1968). The curve

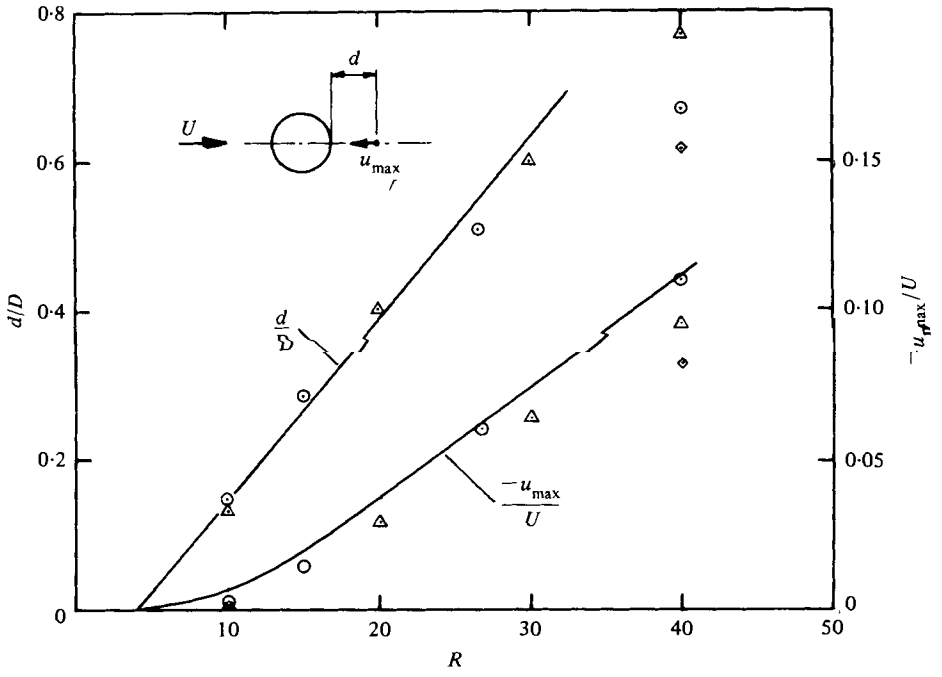

FIGURE 3. Magnitude and location of reverse velocity on centreline of closed wake bubble. Experimental results: ——, Coutanceau & Bouard (1977). Numerical solutions: ○, this study; △, Nieuwstadt & Keller (1973); ◇, Apelt (1958).

shown as the result of Collis & Williams is their curve of best fit to the data for $0{\cdot}02 < R < 44$, i.e.

$$Nu(T'_m/T'_\infty)^{-0{\cdot}17} = 0{\cdot}24 + 0{\cdot}56R^{0{\cdot}45} \tag{10}$$

with T'_m/T'_∞ set to unity. T'_m is the arithmetic mean of the temperature of the cylinder T'_w and that of the approaching fluid T'_∞. The ratio T'_m/T'_∞ accounts to a large extent for the effects of temperature on fluid properties in the correlations of Collis & Williams and it is appropriate to set it to unity for comparison with the results of the numerical solutions since, in both sets, the fluid properties were treated as being unaffected by temperature. It can be seen from figure 4 that the values of Nu obtained from the two different sets of numerical solutions are in close agreement; the values of Nu agree within less than 1% except at $R = 1$ where the difference is still only 5%. The numerical methods used in producing the two sets of results are quite different and the close agreement between the results provides strong evidence for the accuracy of the values of Nu obtained by each of them. Both sets of results give larger values of Nu than indicated by the correlation of Collis & Williams. In the range $5 \leqslant R \leqslant 26{\cdot}67$, our values for Nu are between 3 and 5% larger than the corresponding 'best-fit' value of Collis & Williams and at $R = 1$ and 40 our result is 8% larger. Such agreement with experimental results seems to be about as close as one could realistically hope for when the limitations of the mathematical model are taken into account.

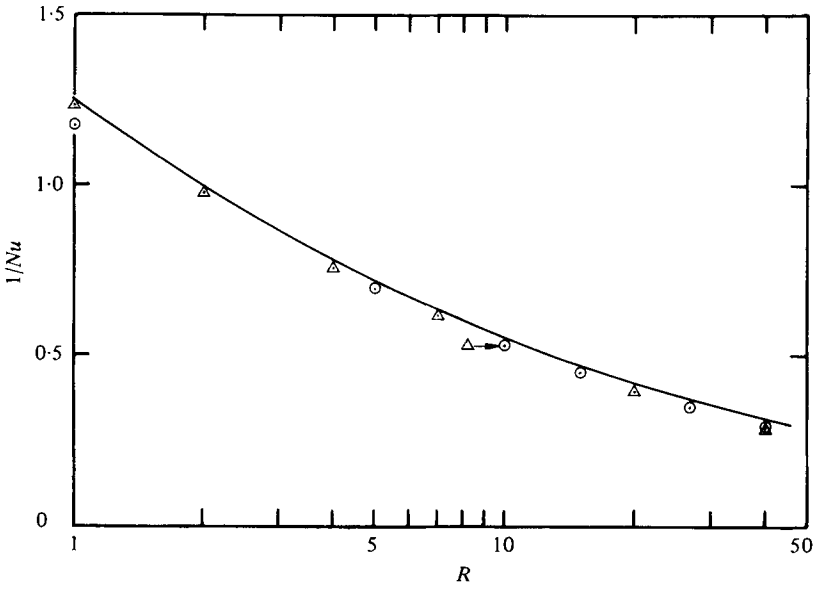

FIGURE 4. Variation of average Nusselt number with Reynolds number. Experimental results: ——, Collis & Williams (1959). Numerical solutions: ⊙, this study; △, Dennis, Hudson & Smith (1968).

4.3. *Unsteady flows*

Impulsive starts from rest. Some of the results obtained for impulsive starts from rest are shown in figure 5. The two cases correspond to final steady state values of R of 5 and 26·67. The results in figure 5 were obtained at the coarser discretization corresponding to $n = 10$, as discussed in § 3.4, and their accuracy is not as good as that of the rest of our results. They are presented here because they provide some useful qualitative information. In both cases, all three drag coefficients pass through a minimum followed by a local maximum before they settle down to a monotonic decay to steady state values. The initial oscillations are sensitive to the discretization used, as has been demonstrated by Ingham (1968), but at later times the monotonic decay is similar to that described by other authors, e.g. Thoman & Szewczyk (1969).

In contrast, Nu decays monotonically from its initial large value throughout the whole of the transient, in both cases. Just before the flow is started impulsively the fluid everywhere is at the temperature of the fluid at $r \to \infty$ and, theoretically, the initial value of Nu at the beginning of motion is infinitely large. However, the finite mesh length 'smears out' the infinitely large gradient of T at the surface of the cylinder to produce a finite gradient over one mesh length. The initial value of $\partial T/\partial r$ at $r = 1$ and the initial value of Nu are, therefore, dependent on the spatial discretization and on the method used for calculating $\partial T/\partial r$. In our computations it is $3n/\pi$.

Impulsive increases in velocity. The responses of drag forces and of heat transfer to impulsive increases in velocity of 50% from initial values of R of 1, 10 and 26·67 are shown in figure 6. The quantities plotted in figure 6 have been normalized with respect to the steady state values they had at the initial, lower Reynolds number. In all cases each of the drag coefficients, C_{Dt}, C_{Dp} and C_{Df}, decreases from its value corresponding to the initial steady state as soon as the increase of velocity is imposed,

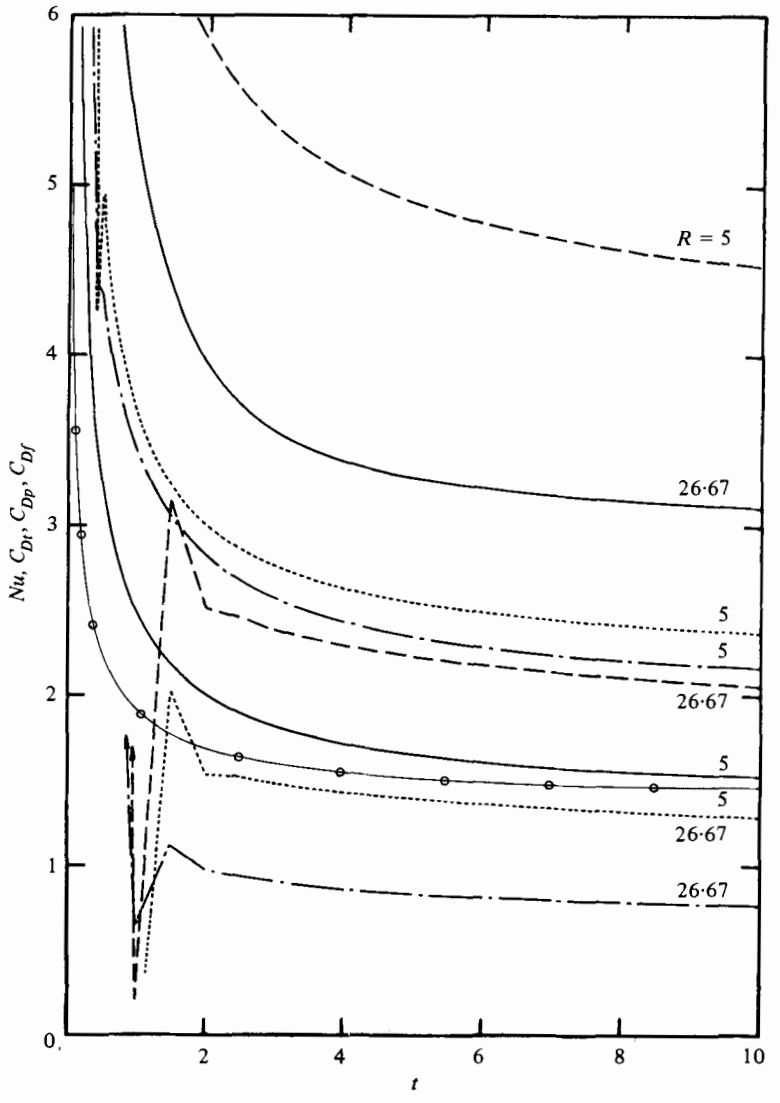

FIGURE 5. Variation with time of Nusselt number and of drag coefficients for impulsive starts from rest to Reynolds numbers of 5 and 26·67: ——, Nu; – – –, C_{Dt}; · · ·, C_{Dp}; – · –, C_{Df}; -⊖-⊖-, Nu for sudden increase in temperature at $R = 5$.

in proportion to $1/R$. Thereafter, the effects of viscosity adjust the velocity field to that appropriate to the new, larger value of R and each drag coefficient increases monotonically to approach its final steady state value asymptotically. In contrast, the impulsive change in flow velocity does not produce an instantaneous change in Nu since the temperature in the vicinity of the cylinder is not changed instantaneously and it responds smoothly to the effects of changes in the velocity field as these develop after the impulse is applied. Consequently, Nu increases monotonically throughout the transient, showing initially a relatively rapid rate of increase followed at a later time by an asymptotic approach to the new steady state value.

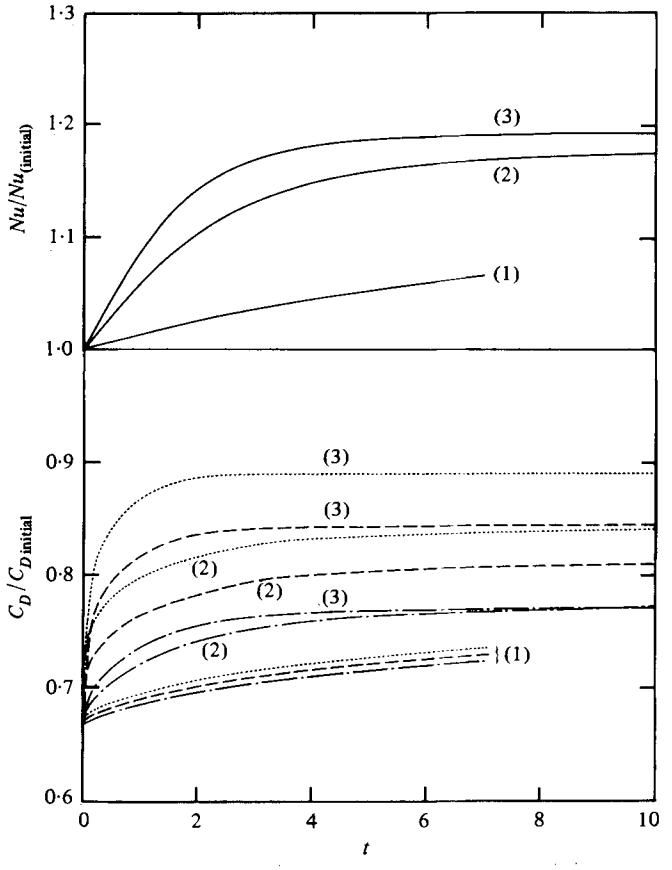

FIGURE 6. Responses of drag forces and of heat transfer to impulsive increases in velocity of 50%; (1) $R = 1 \rightarrow 1{\cdot}5$; (2) $R = 10 \rightarrow 15$; (3) $R = 26{\cdot}67 \rightarrow 40$. ——, Nu; – – –, C_{Dt}; · · ·, C_{Dp}; – · –, C_{Df}.

The speed of response to the disturbance of all quantities increases with the value of R of the initial flow state and, at each value of R, the drag coefficients respond more rapidly than does the heat transfer. An indication of these relative speeds is given by the magnitudes of the 'time constant' τ, which is used here as the time taken for the response to reach 0·63 of the increment to the final value. In order corresponding to initial values of R of 1, 10 and 26·67 the values of τ for C_{Dt} are 4·4, 0·86 and 0·38, respectively, while the values of τ for Nu are 6·7, 2·33 and 1·61, respectively.

The results presented in figures 5 and 6 provide justification for the use in hot-wire anemometry of steady state heat transfer relations, since the thermal transients which result from step changes in velocity in the range of R studied have time scales of order $10a/U$ or less and this is much less than any other time scale encountered in practical anemometry.

Preliminary computations showed that a time step for numerical integration determined in accordance with § 3.4 was satisfactory for the case when R increases from 1 to 1·5. However, when the other two cases were computed with the corresponding time step, small oscillations in C_{Dp} occurred during the early part of the transient. A reduction of the time step to half the value indicated in § 3.4 in these two

cases resulted in completely smooth responses. In order to test further the sensitivity of the transients to the length of time step used in the numerical integration, each of the cases was recomputed through the early part of the transient with the time step set at one half that indicated above. The response curves for drag coefficients were only slightly affected by this halving of the time step and, when the origin of time was set at the end of the first time step rather than at the beginning, the curves became virtually identical. For this reason the origin of time for the curves of drag coefficients in figure 6 has been set at the end of the first time step. On the other hand, the response curves for Nu were virtually identical for all stable time steps, without adjustment of the origin of time.

Periodic fluctuations in velocity. The effects on drag and on heat transfer of a periodic fluctuation in the magnitude of the flow velocity are shown in figure 7. The velocity fluctuation imposed was a sinusoidal variation of amplitude 10 %, about a mean flow at $R = 10$ to give a range of R from 9 to 11. The angular frequency, $1/2{\cdot}3$, was chosen to be approximately the reciprocal of the time constant for the heat transfer response. The temperature of the cylinder was maintained constant throughout. The calculated response curves are compared in figure 7 with curves which show the steady state values of the quantities associated with the instantaneous value of R; these latter will be referred to as the 'quasi-steady' response curves. It is noted that even these quasi-steady response curves are not sinusoidal because the drag and heat transfer are not linear functions of R. All of the calculated responses exhibit a small decaying transient resulting from the initial instantaneous change from steady flow to the fluctuating flow but this has virtually disappeared after the first half period and, thereafter, the calculated response is very nearly periodic, as shown by the summary in table 1, which lists the amplification of the response at the successive stationary values, relative to the quasi-steady response.

The response of each of the three drag coefficients to the velocity fluctuations is larger in amplitude than the corresponding quasi-steady response and the response leads the velocity fluctuation. The magnitudes of the phase lead, calculated from the average of the last three crossings in figure 7, are 12·05°, 14·2° and 10·1° for C_{Dt}, C_{Dp} and C_{Df}, respectively. In contrast, the heat transfer response is smaller in amplitude than the corresponding quasi-steady response and lags the velocity fluctuation, the phase lag averaged over the last three crossings being 41·1°. It is interesting to compare this result with that obtained by Davies (1976) for $R \ll 1$ by means of an Oseen type of solution. He found that, at low frequencies, the fluctuating component of heat transfer is in phase with the velocity, the magnitude being given by the result for steady heat transfer but that, at high frequencies, the heat transfer lags the velocity by $\frac{1}{2}\pi$, the relative magnitude of heat transfer decreasing as (frequency)$^{-1}$. Davies estimated that the minimum value of the Strouhal number of the impressed fluctuations at which time derivatives become important is $\sim 0{\cdot}1RPr$. Applied to the case we have calculated, this gives a minimum Strouhal number of 0·7 while the frequency of our calculations corresponds to a Strouhal number of 0·87. Thus, even though our calculations were done about $R = 10$, it appears that the response is generally consistent with that implied by the analysis of Davies for intermediate frequencies at $R \ll 1$.

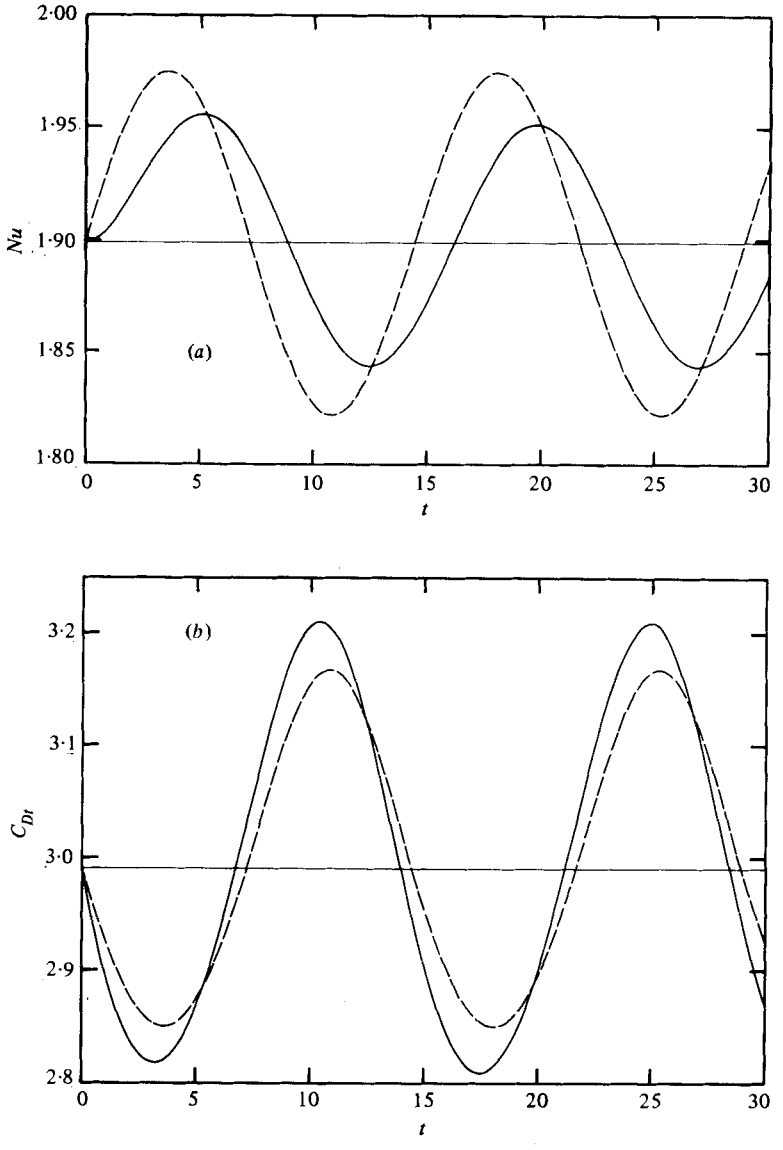

FIGURE 7. For legend see facing page.

Order of stationary value	Amplification factor			
	C_{Dt}	C_{Dp}	C_{Df}	Nu
First	1·224	1·280	1·180	0·751
Second	1·245	1·236	1·266	0·712
Third	1·295	1·334	1·228	0·698
Fourth	1·244	1·236	1·264	0·718

TABLE 1. Amplification at successive stationary values in response to sinusoidal velocity fluctuation.

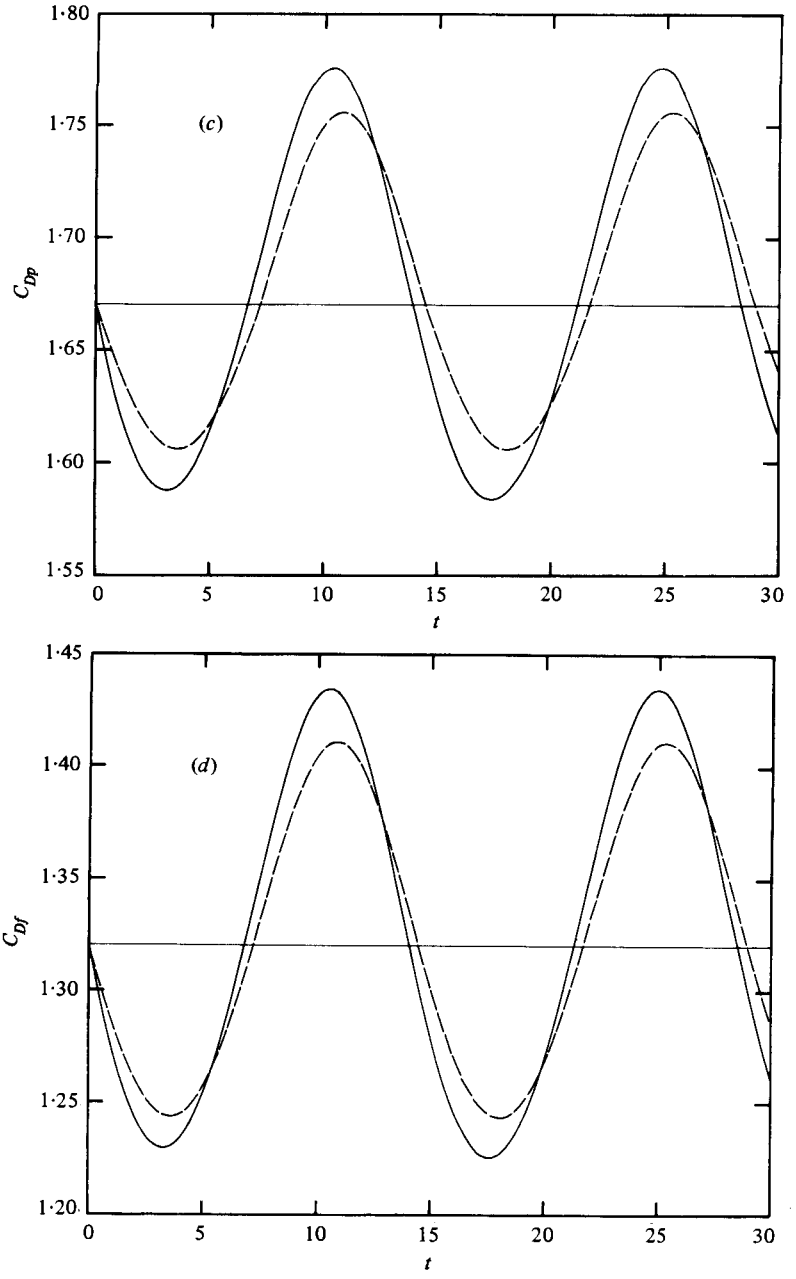

FIGURE 7. Responses of drag forces and of heat transfer to periodic fluctuation in velocity about a mean flow at $R = 10$: (*a*) Nusselt number; (*b*) total drag coefficient; (*c*) pressure drag coefficient; (*d*) friction drag coefficient. ——, computed response; – – –, 'quasi-steady' response.

4.4. *Instantaneous increase in temperature of cylinder*

The response of heat transfer when the temperature of the cylinder is increased instantaneously was computed for steady flows at $R = 1$, 5 and 40. Since the fluid properties have been assumed invariant with temperature, the equation (3*a*) is linear in T and the results are shown in figure 8 in the form $(Nu(t) - Nu(0))/(\Delta T_w Nu(0))$,

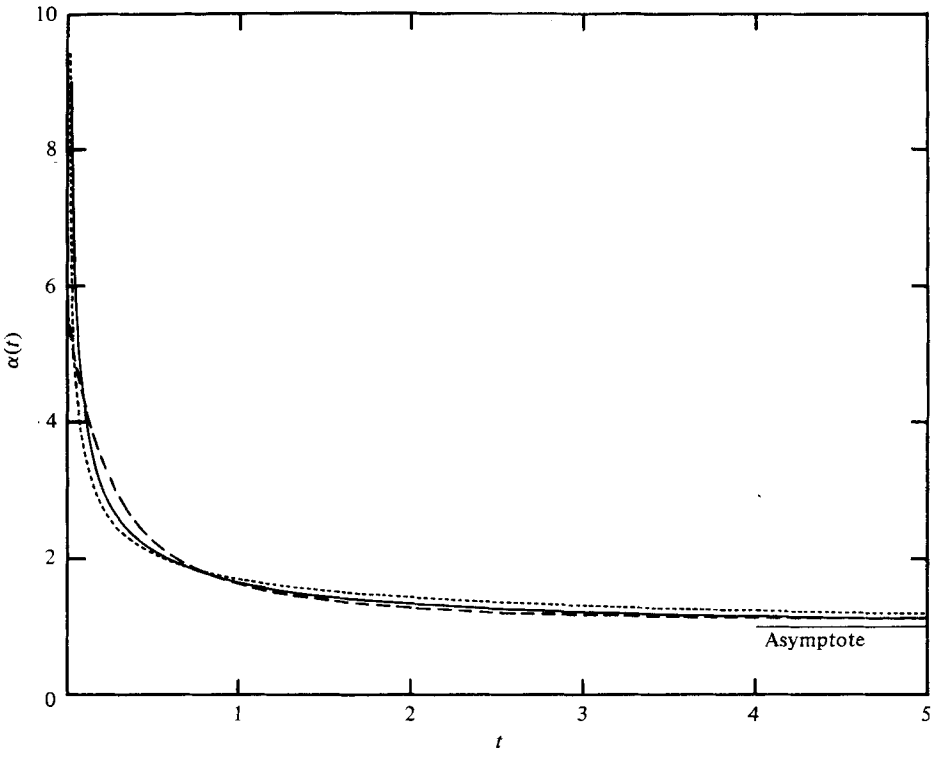

FIGURE 8. Response of heat transfer to an instantaneous increase in the temperature of the cylinder. - - -, $R = 1$; ——, $R = 5$; – – –, $R = 40$.

denoted by $\alpha(t)$, which expresses the increase in heat transfer from the initial steady state value per unit of increase in the temperature of the cylinder, as a proportion of the initial steady state value. ΔT_w denotes the increase in the temperature of the cylinder. The asymptotic value of $\alpha(t)$ for $t \to \infty$ is unity. The initial value of $\alpha(t)$ is, theoretically, infinite but the finite mesh length 'smears out' the initial, infinitely large gradient of T at the surface of the cylinder to produce a finite gradient over one mesh length. Consequently, the initial value of $\alpha(t)$ is dependent on the spatial discretization and also on the method used for numerical differentiation. In our case, the initial value of $(Nu(t) - Nu(0))/\Delta T_w$ is 19·1 in each case but the initial value of $\alpha(t)$ varies because $Nu(0)$ varies with R.

The response curves in figure 8 all show an initial rapid decay followed by a slow asymptotic approach to the final steady state. At the beginning of the transient, diffusion predominates and, as can be predicted from equation (3a), the decay rate is nearly proportional to $1/R$. At later times, the effects of diffusion become much smaller, convection becomes proportionately more important; the decay rates are small and, for $t > 2$, their magnitudes increase with R.

The transients of heat transfer for this case of an instantaneous increase in the temperature of the cylinder are similar in shape to those associated with the impulsive start up from rest of the flow past a cylinder which is held at a constant temperature. To illustrate this similarity, the response to the instantaneous increase in temperature

of a cylinder in steady flow at $R = 5$ is also shown in figure 5, with the Nusselt number calculated with reference to the new temperature of the cylinder. The resemblance to the case of impulsive start-up to $R = 5$ is apparent.

5. Closure

The results of the numerical solutions presented here provide new information about heat transfer from a heated cylinder in unsteady flows and, in our discussion, we have concentrated on those matters considered to be of interest from the view point of the fluid dynamics. The application of these results to the analysis and design of constant resistance hot-wire anemometers is dealt with by Bullock & Ledwich (1973).

The authors gratefully acknowledge the financial support received from the Australian Research Grants Committee. The computer time was granted by The Australian Institute of Nuclear Science which provided for access to the computer of the Australian Atomic Energy Commission.

REFERENCES

Apelt, C. J. 1958 *Aero. Res. Counc. R. & M.* 3175.

Arakawa, A. 1966 *J. comp. Phys.* **1**, 119.

Batchelor, G. K. 1967 *An Introduction to Fluid Dynamics*. Cambridge University Press.

Bullock, K. J. & Ledwich, M. A. 1973 *Mech. Eng. Res. Rep.* no. 2/73. University of Queensland.

Cole, J. & Rosko, A. 1954 *Proc. of Heat Transfer and Fluid Mech. Inst.*, p. 13. Stanford University Press.

Collins, W. M. & Dennis, S. C. R. 1973 *J. Fluid Mech.* **60**, 105.

Collis, D. C. & Williams, M. J. 1959 *J. Fluid Mech.* **6**, 357.

Coutanceau, M. & Bouard, R. 1977 *J. Fluid Mech.* **79**, 231.

Davies, H. G. 1976 *J. Fluid Mech.* **73**, 49.

Dennis, S. C. R. & Chang, G. Z. 1970 *J. Fluid Mech.* **42**, 471.

Dennis, S. C. R., Hudson, J. D. & Smith, N. 1968 *Phys. Fluids* **11**, 933.

Hieber, C. A. & Gebhart, B. 1968 *J. Fluid Mech.* **32**, 21.

Hodnett, P. F. 1969 *J. Fluid Mech.* **39**, 465.

Illingworth, C. R. 1963 In *Laminar Boundary Layers* (ed. L. Rosenhead), p. 193. Clarendon Press.

Imai, I. 1951 *Proc. Roy. Soc.* A **208**, 487.

Ingham, D. B. 1968 *J. Fluid Mech.* **31**, 815.

Kassoy, D. R. 1967 *Phys. Fluids* **10**, 938.

Kawaguti, M. 1953 *J. Phys. Soc. Japan* **8**, 747.

Keller, H. B. & Takami, H. 1966 *Numerical Solutions of Nonlinear Differential Equations* (ed. D. Greenspan), p. 116. Wiley.

Levey, H. 1959 *J. Fluid Mech.* **6**, 385.

Nieuwstadt, F. & Keller, H. B. 1973 *Computers & Fluids* **1**, 59.

Payne, R. B. 1958 *J. Fluid Mech.* **4**, 81.

Takaisi, Y. 1969 *Phys. Fluids Suppl.* **12**, II 86.

Takami, H. & Keller, H. B. 1969 *Phys. Fluids Suppl.* **12**, II 51.

Thoman, D. C. & Szewczyk, A. A. 1969 *Phys. Fluids Suppl.* **12**, II 76.

Tritton, D. J. 1959 *J. Fluid Mech.* **6**, 547.

Wood, W. W. 1968 *J. Fluid Mech.* **32**, 9.